Molecular dynamics simulation on the interaction between single-walled carbon nanotubes and binaphthyl core-based chiral phenylene dendrimers

Zunli Mo,[a] Xiaobo Zhu, Guorui Wang, Weiwei Han, and Ruibin Guo
Key Laboratory of Eco-Environment-Related Polymer Materials, Ministry of Education of China, Lanzhou 730070, China; Key Laboratory of Polymer Materials of Gansu Province; and College of Chemistry and Chemical Engineering, Northwest Normal University, Lanzhou 730070, China

(Received 17 April 14; accepted 14 August 14)

Single-walled carbon nanotubes (SWCNTs), which have a unique electronic structure, nanoscale diameter, high curvature, and extra-large surface area, are ideal for making a new class of nanocomposites. In this study, under the condensed phase optimized molecular potentials for atomistic simulation studies force field, classical molecular dynamics simulation is used to study the molecular interactions between SWCNTs and the molecules of binaphthyl core-based chiral phenylene dendrimers (G0–G2). The simulation results revealed that both G2 and G1 molecules have obvious attractive interactions with SWCNTs, and theoretically demonstrated the possibility of noncovalent functionalization of SWCNTs with chiral dendrimers. The influence of temperature on composites was also studied, and the results indicate that the interaction decreases strongly for SWCNTs@G1 and SWCNTs@G2 with increasing temperature. The possibility during real-world composite processing would create the desired structure bridges between nanotubes and chiral dendrimers, which can be used to produce nanocomposites such as highly sensitive as well as enantioselective fluorescent sensors.

I. INTRODUCTION

Since their discovery in 1991, carbon nanotubes (CNTs) have attracted great attention due to their marvelous properties, such as excellent stiffness against bending, high electrical conductivity, and tensile strength. Nowadays, CNTs are considered to be the most promising class of systems for the development of applications in the field of nanotechnology.[1–3] Polymer materials reinforced with nanoparticles (e.g., nanosphere, nanotube, clay platelet) have recently received tremendous attention in both scientific and industrial communities with their extraordinary enhanced properties.[4–9] Therefore, single-walled carbon nanotube (SWCNT) based polymer nanocomposites are of considerable current interest to scientists and engineers because of their unique physical and mechanical properties that are not attainable with conventional composites.[10,11]

CNTs can be functionalized covalently or noncovalently for improved dispersion in matrix. Covalent functionalization introduces atomic defects and internal stresses into the nanotubes, which thereby deteriorates their mechanical properties.[12,13] Therefore, it is desirable to explore the possibility of optimizing noncovalent intermolecular interactions between CNTs and polymers in view of achieving strong interfacial binding in a system.[14–19] In the case of nonfunctionalized SWCNTs@polymer composites, the nature of interfacial bonding energy comes from electrostatic and van der Waals force in the composite system. The strength of the interfacial binding depends on the geometrical conformation of the polymers with respect to the nanotube. Hence, chiral dendrimers are selected for the simulation of SWCNTs@dendrimer nanocomposites.

Dendrimers, which are considered as a new class of polymer and possess many interesting and unique properties, are hyperbranched macromolecules. However, dendrimers are different from many classical polymers, such as linear and branched polymers, in which they are well defined, with a high degree of molecular uniformity and monodispersity, as well as a highly functional surface. Low generation dendrimers have an open structure in a general way, but the structure becomes more globular and dense as the generation increases. One of the most synthetically challenging areas in the field of dendrimer chemistry is preparation of chiral dendrimers,[20–25] which open the possibility to study the effect of the chirality in macromolecular systems. In addition, potential applications of chiral dendrimers, e.g., molecular recognition,[23] sensor technology,[24,25] and catalyst[20,21] have been investigated in detail. In spite of these exciting observations through experimental methods, the mechanism of interactions between chiral dendrimers and

[a]Address all correspondence to this author.
e-mail: mozlnwnu2010@163.com
DOI: 10.1557/jmr.2014.237

 © Materials Research Society 2014

https://doi.org/10.1557/jmr.2014.237 Published online by Cambridge University Press

SWCNTs remains unclear. Molecular dynamics (MD) simulation is a powerful tool which allows one to examine properties that are not accessible to experimental approaches. Here, MD simulation is used to investigate the interaction between binaphthyl core-based chiral phenylene dendrimers[26] and SWCNTs.

II. SIMULATION DETAILS

A. Computational method

Here, MD simulations were carried out with a commercial software package called Materials Studio developed by Accelrys Inc. The condensed phase optimized molecular potentials for atomistic simulation studies (COMPASS) module in the Materials Studio software was used to conduct force-field computations.[22] The COMPASS was a parameterized, tested, and validated first ab initio force field, which enables an accurate prediction of various gas phase and condensed phase properties of most of the common organic and inorganic materials.[27] And the MD simulation for each case study was performed long enough to observe several cycles of thermal vibration. The interval of each MD simulation step was typically 1 fs. All calculations were carried out at the initial temperature of 298 K except special conditions, using NVT ensemble.

B. Force field

As we know, the main goal of simulations of the systems containing a large number of particles is generally to obtain the systems' bulk properties which are primarily controlled by the location of atomic nuclei, so the knowledge of the electronic structure that provided by the quantum mechanic techniques is not critical. Thus, we could have good insight into the behavior of a system if reasonable, physically based approximation of the potential (force-field) can be obtained, which can be used to generate a set of system configurations which are statistically consistent with a fully quantum mechanical description. A force field in molecular mechanics and MD is the average description of the existing interactions among various atoms in a molecule or a group of molecules in terms of function and parameter sets. As stated above, a crucial point in the atomistic simulations of multiparticle systems is the choice of the force fields, a brief overview of which is given in this section. In general, the nonbond energy of a molecular system includes the following term[28]:

$$E_{\text{nonbond}} = E_{\text{vdW}} + E_{\text{Coulomb}} + E_{\text{H-bond}} \quad . \qquad (1)$$

The nonbond interaction term, E_{nonbond}, accounts for the interactions between nonbonded atoms and includes the van der Waals energy (E_{vdW}), the Coulomb electrostatic energy (E_{Coulomb}), and the hydrogen bond energy ($E_{\text{H-bond}}$). The COMPASS force field uses expressions for E_{Coulomb} and E_{vdW} as follows[29,30]:

$$E_{\text{Coulomb}} = \sum_{i>j} \frac{qiqj}{\in rij} \quad , \qquad (2)$$

$$E_{\text{vdW}} = \sum_{i>j} \left[\frac{Aij}{rij9} - \frac{Bij}{rij6} \right] \quad , \qquad (3)$$

where q is the atomic charge, $\in$ is the dielectric constant, and r_{ij} is the i–j atomic separation distance. A_{ij} and B_{ij} are fitted from quantum mechanics calculations and are implemented into the Discover module of Materials Studio, a powerful commercial atomic simulation program used in this study.

C. Molecular model

1. Molecular model of a (10,10) SWCNT

To simulate the interactions between CNTs and G0–G2, an armchair SWCNTs and three chiral dendrimer models are selected as the representative elements for the simulation. Initially, the dendrimers G0–G2 were put near the middle of SWCNTs in a distance of about 9.5 Å within the cutoff distance of van der Waals interactions. The dimensions of the simulation cell were maintained as 50 Å × 50 Å × 50 Å. In this study, the molecular model of a (10,10) SWCNT was established using Materials Studio. The electronic structure of the carbon atoms in the SWCNT model was sp^2 hybridization. The modeled SWCNTs had a finite length of 9.7 nm with a diameter of 1.38 nm. The computer graphics picture of the SWCNT model is shown in Fig. 1.

The unsaturated boundary effect was avoided by adding 20 hydrogen atoms at each end of the SWCNT. The model had 400 carbon atoms and 40 hydrogen atoms. C–C and C–H bond length was 1.42 and 1.10 Å, respectively. The hydrogen atoms had charges of +0.1268 e, and the carbon atoms connecting hydrogen atoms had charges

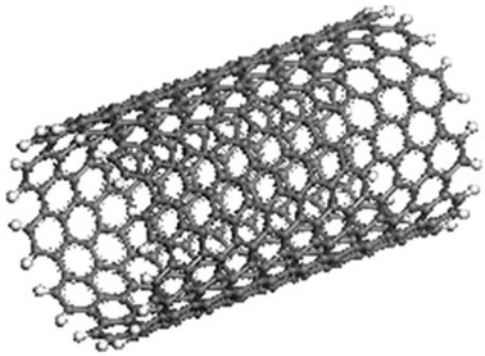


FIG. 1. Molecular model of a (10,10) SWCNT.

https://doi.org/10.1557/jmr.2014.237 Published online by Cambridge University Press

of −0.1268 e, thus the SWCNT was neutrally charged. This model was used for molecule interactions.

2. Molecular model of the investigated chiral dendrimers

The simulated chiral dendrimers (G0, G1, G2) were binaphthyl core-based chiral phenylene dendrimers. The chemical structures and molecular models of G0–G2 are provided in Figs. 2 and 3.

To make a direct and comparable measurement of the interaction energies between SWCNTs and chiral dendrimers, the simulated models of G0–G2 were selected with comparable numbers of atoms and molecular weights (G0: 76 atoms, 590.722; G1: 156 atoms, 1199.51; and G2: 315 atoms, 2416.07). The number of atoms and monomers is small (about 182 atoms per molecule, which corresponds to 2 monomers for G0, 1 monomer for G1, and half a monomer for G2), and the results of our simulation describe the behavior of the small part of the whole composites.

Energy-minimization molecular mechanics were performed using Materials Studio to find the thermal stable morphology and achieve a conformation with minimum potential energy for the chiral dendrimers. This minimum energy conformation of the molecule was used as initial status in the following MD computation. As shown in Figs. 2 and 3, the chiral dendrimers were twisted to achieve a low potential energy.

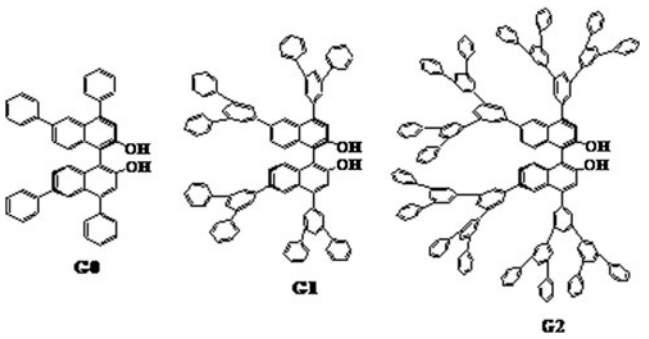


FIG. 2. Chemical structure of G0–G2.

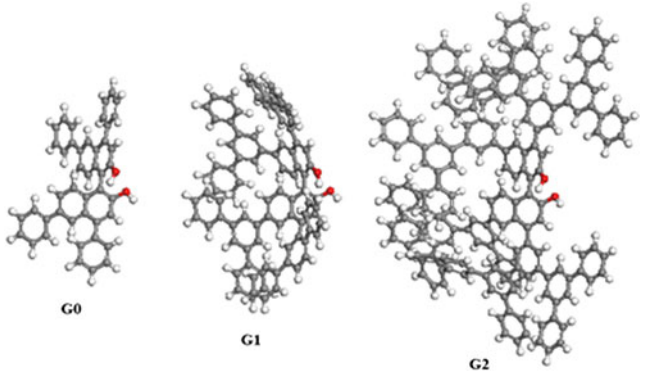


FIG. 3. Molecular models of G0–G2.

III. RESULTS AND DISCUSSION

Figure 4 shows the snapshots of dendrimers and SWCNTs observed before and after the simulation.

The simulation showed that the three dendrimers would stretch and move toward the nanotube until they finally wrapped on the surface of the helix of the nanotube, and the equilibrium was achieved at last. Particularly, the aromatic rings of G0–G2 orientated to align their ring planes parallel to the SWCNT surfaces during the MD simulations, which may be related to the π–π interactions between the aromatic rings and the SWCNTs, and the strong polarity of dendrimers cannot be neglected.

In the case of nonbond SWCNTs@polymer composites, the nature of interfacial bonding energy comes from electrostatic and van der Waals force in the composite system. Generally, the interaction energy is estimated from

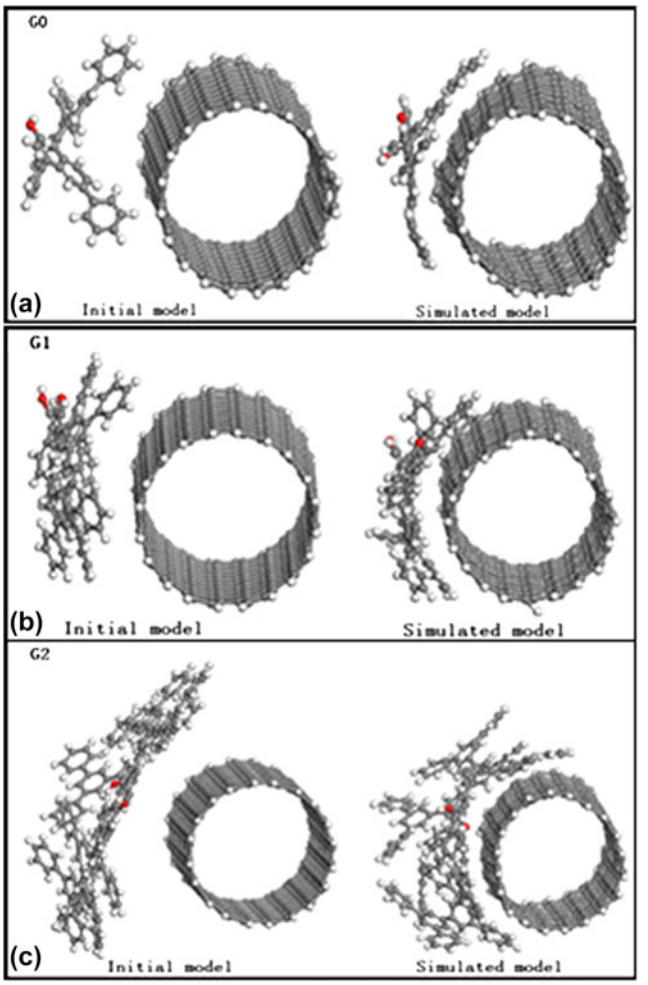


FIG. 4. The initial and simulated models of the composite (a) for G0, (b) for G1, (c) for G2.

https://doi.org/10.1557/jmr.2014.237 Published online by Cambridge University Press

the difference between the potential energy of the composite system and the potential energies for the polymer molecules and the corresponding SWCNTs as follows:

$$\Delta E = E_{\text{total}} - (E_{\text{SWCNTs}} + E_{\text{dendrimer}}) \quad , \qquad (4)$$

where E_{total} is the total potential energy of the composite, E_{SWCNTs} is the energy of the CNT without the dendrimer, and $E_{\text{dendrimer}}$ is the energy of the dendrimer without the nanotube. In other words, the interaction energy can be calculated as the difference between the minimum energy and the energy at an infinite separation of the CNT and the dendrimer matix.[31–33]

Figure 5 shows the energy evolution of SWCNTs@dendrimer (G0–G2) composites, including total energy, potential energy, and kinetic energy. The kinetic energy was almost the same for the three dendrimers, and SWCNTs@G0 has the lowest potential energy and total energy. Figure 6 shows the total energy at different temperatures during the simulation and we can find that the total energy of SWCNTs@dendrimer (G0–G2) has the same tendency to rise during the simulation, and obviously SWCNTs@G2 has the highest total energy while SWCNTs@G0 has the lowest total energy at the same temperature. Figure 7 shows the interaction during the wrapping process for SWCNTs@dendrimer (G0–G2) composites at the very beginning of the simulations. For SWCNTs@G0 and SWCNTs@G1, the attractive interaction increases respectively to −50 and −90 kcal/mol, while for SWCNTs@G2 it increases to −140 kcal/mol, which is much stronger. Both SWCNTs@G1 and SWCNTs@G2 are molecules with more groups of aromatic rings in the backbone, so the interaction energy between chiral dendrimers and SWCNTs may be greatly influenced by aromatic rings, and related to the delocalized π-bonds on the SWCNTs due to sp^2 hybridization with π-bonds of aromatic rings. Thus, the interaction is mainly based on van der Waals forces or π–π stacking.

To assess the temperature dependence of the intermolecular interaction between the dendrimers and SWCNTs, MD simulations were carried out at different temperatures. The temperature was varied between 298 and 548 K in steps of 25 K. Figure 8 shows the temperature dependence of the intermolecular interaction. It was shown that the interaction decreases weakly with increasing temperature for SWCNTs@G0, so the temperature influence is neglectable. However, the interaction decreases strongly with increasing temperature for SWCNTs@G1 and SWCNTs@G2, which may be caused by the aromatic rings and geometrical conformation of the dendrimers.

For analysis of specific interactions, radial distribution function (RDF) was examined to research the system. Figure 9 shows the RDF curves for the pairs of atoms in

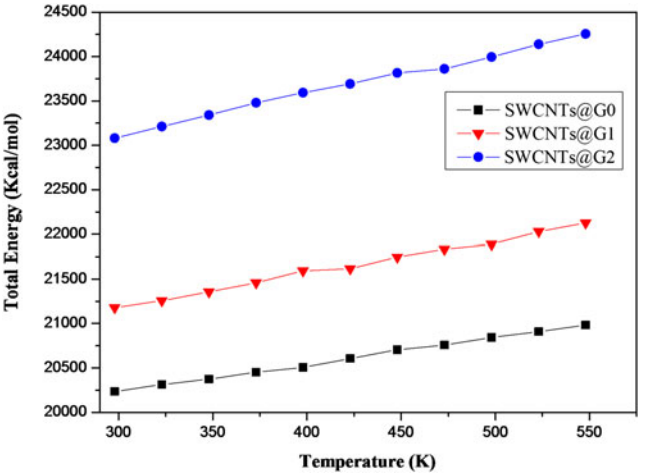


FIG. 6. Total energy evolution for SWCNTs@dendrimer (G0–G2) composites at different temperatures.

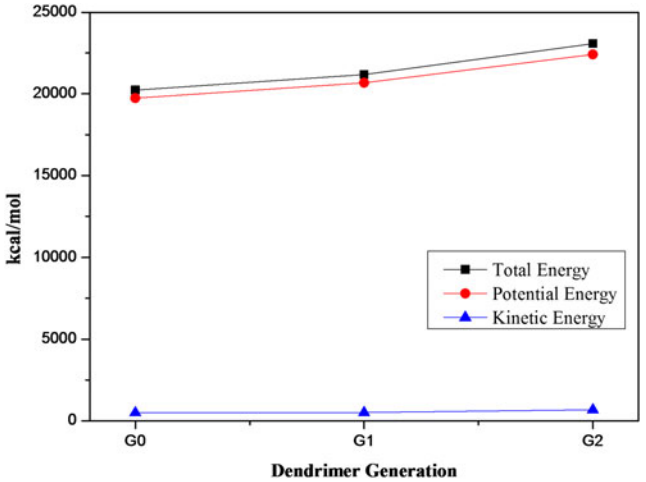


FIG. 5. Energy evolution of SWCNTs@dendrimer (G0–G2) composites.

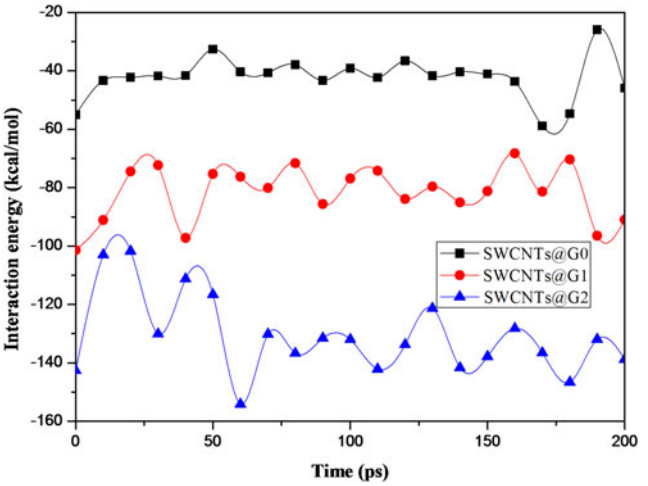


FIG. 7. Interaction energy evolution for SWCNTs@dendrimer (G0–G2) composites during 200 ps simulation.

https://doi.org/10.1557/jmr.2014.237 Published online by Cambridge University Press

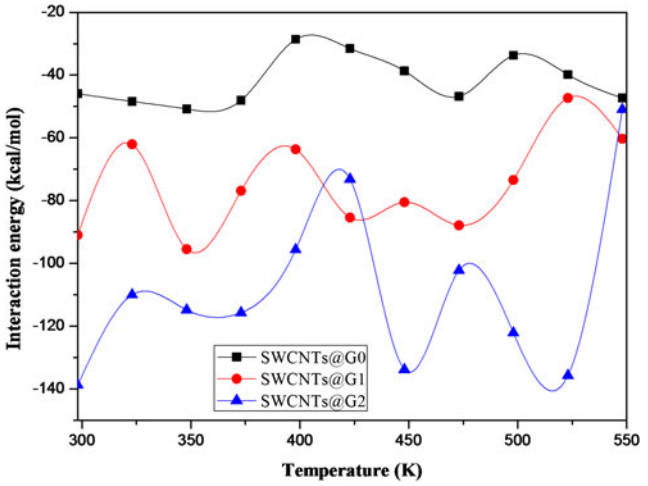


FIG. 8. Intermolecular interaction as a function of temperature.

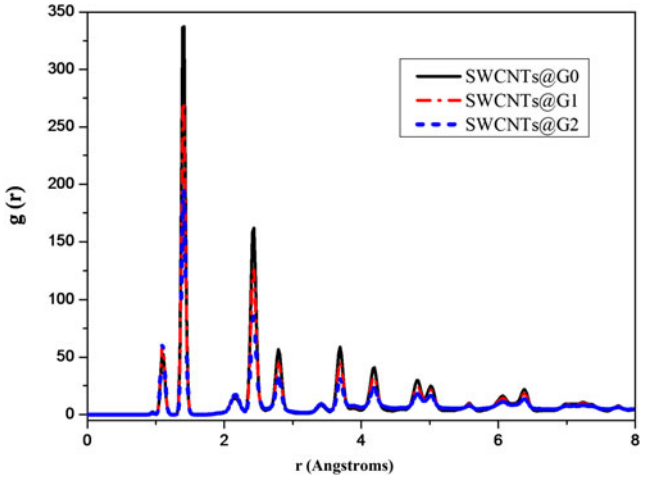


FIG. 9. RDF curves for SWCNTs@dendrimer (G0–G2) molecules.

the SWCNTs@dendrimer (G0–G2) molecules. It can be clearly seen that the RDF for these three cases is almost identical except that SWCNTs@G0 has the longest peak while SWCNTs@G2 has the shortest. Meanwhile, there is a sharp peak at about $R = 1.3$ Å, which is attributed to chemical bonds of dendrimer chain itself, and this result shows the highest probability for strong interaction in the system. The other two smaller peaks appear at $R = 2.7$ Å and $R = 3.7$ Å which is mainly caused by intra- and intermolecular interaction in nonbonding interaction. Thus, the probability for the distance of 1.3 Å is a balance distance for the electrostatic interaction of these composite materials because of their contrary charges, which could make the composite combination effectively. And theoretically demonstrated the possibility of noncovalent functionalization of SWCNTs with chiral dendrimers.

IV. CONCLUSION

In this study, the molecular interactions between SWCNTs and the molecules of chiral dendrimer G0–G2 were conducted with MD simulation. The simulation results revealed that both G2 and G1 molecules have obvious attractive interactions with SWCNTs. The results also show that the aromatic ring structures of G0–G2 aligned the aromatic ring planes toward the SWCNT surface and wrapped around it, mainly depend on the delocalized π-bonds on the SWCNT wall due to sp^2 hybridization with π-bonds of aromatic rings. The temperature influence is neglectable for G0 but strong for G1 and G2.

The results theoretically demonstrated the possibility of noncovalent functionalization of SWCNTs with chiral dendrimers. The possibility of noncovalent functionalization of SWCNTs with chiral dendrimers during real-world composite processing would create the desired structure bridges between nanotubes and chiral dendrimers, which can be used to produce nanocomposites such as highly sensitive as well as enantioselective fluorescent sensors, due to dendritic arms of G0–G2, which might have contributed to their chiral optical effects probably because of the increased steric interaction between the adjacent arylene units in the dendrons, and for G0–G2 the optically active binaphthyl cores lead to enantioselective recognition of the chiral substrates. These sensors will be useful in the high throughput combinatorial chiral catalyst screening.

ACKNOWLEDGMENTS

The authors are grateful for financial aid from the National Natural Science Foundation of China (51262027), the financial support from the Natural Science Foundation of Gansu Province (1104GKCA019 and 1010RJZA023), Science and Technology Tackle Key Problem Item of Gansu Province (2GS064-A52-036-08), and the fund of the State Key Laboratory of Solidification Processing in NWPU (SKLSP201011).

REFERENCES

1. X. Lu and Z-F. Chen: Curved pi-conjugation and the related chemistry of small fullerenes (smaller than C_{60}) and single-wall carbon nanotubes. *Chem. Rev.* **105**, 3643 (2005).
2. P.M. Ajayan: Nanotubes from carbon. *Chem. Rev.* **99**, 1787 (1999).
3. X-S. Qi, J-L. Xu, W. Zhong, C-T. Au, and Y-W. Du: Controllable synthesis, characterization, and magnetic properties of magnetic nanoparticles encapsulated in carbon nanocages and carbon nanotubes. *Diamond Relat. Mater.* **45**, 12 (2014).
4. R. Krishnamoorti and R.A. Vaia: *Polymer Nanocomposites: Synthesis, Characterization, and Modeling* (American Chemical Society, Washington DC, 2001); pp. 7–14.

https://doi.org/10.1557/jmr.2014.237 Published online by Cambridge University Press

5. C. Xue, X. Wang, W-Y. Zhu, Q. Han, C-H. Zhu, J-L. Hong, X-M. Zhou, and H-J. Jiang: Electrochemical serotonin sensing interface based on double-layered membrane of reduced graphene oxide/polyaniline nanocomposites and molecularly imprinted polymers embedded with gold nanoparticles. *Sens. Actuators, B* **196**, 57 (2014).
6. A. Shokuhfar, A. Zare-Shahabadi, A.A. Atai, S. Ebrahimi-Nejad, and M. Termeh: Predictive modeling of creep in polymer/layered silicate nanocomposites. *Polym. Test.* **31**(2), 345 (2012).
7. Q-H. Zeng, A-B. Yu, G-Q. Lu, and D.R. Paul: Clay-based polymer nanocomposites: Research and commercial development. *J. Nanosci. Nanotechnol.* **5**, 1574 (2005).
8. S.C. Tjong: Structural and mechanical properties of polymer nanocomposites. *Mater. Sci. Eng., R* **53**, 73 (2006).
9. A. Okada and A. Usuki: Twenty years of polymer-clay nanocomposites. *Macromol. Mater. Eng.* **291**, 1449 (2006).
10. M. Wang, F. Jakubka, F. Gannott, M. Schweiger, and J. Zaumseil: Generalized enhancement of charge injection in bottom contact/top gate polymer field-effect transistors with single-walled carbon nanotubes. *Org. Electron.* **15**(3), 809 (2014).
11. B. Sitharaman, X. Shi, X.F. Walboomers, H. Liao, V. Cuijpers, L.J. Wilson, A.G. Mikos, and J.A. Jansen: In vivo biocompatibility of ultra-short single-walled carbon nanotube/biodegradable polymer nanocomposites for bone tissue engineering. *Bone* **43**(2), 362 (2008).
12. H.D. Wagner: Nanotube–polymer adhesion: A mechanics approach. *Chem. Phys. Lett.* **361**, 57 (2002).
13. Z. Mao, A. Garg, and S.B. Sinnott: Molecular dynamics simulations of the filling and decorating of carbon nanotubules. *Nanotechnology* **10**, 273 (1999).
14. B-Z. Tang and H. Xu: Preparation, alignment, and optical properties of soluble polyphenylacetylene-wrapped carbon nanotubes. *Macromolecules* **32**, 2569 (1999).
15. K. Liao and S. Li: Interfacial characteristics of carbon nanotube-polystyrene composite system. *Appl. Phys. Lett.* **79**, 4225 (2001).
16. M.J. O'Connell, P. Boul, L.M. Ericson, C. Huffman, Y.H. Wang, E. Haroz, C. Kuper, J. Tour, K.D. Ausman, and R.E. Smalley: Reversible water-solubilization of single-walled carbon nanotubes by polymer wrapping. *Chem. Phys. Lett.* **342**, 265 (2001).
17. D.W. Steuerman, A. Star, R. Narizzano, H. Choi, R.S. Ries, C. Nicolini, J.F. Stoddart, and J.R. Heath: Interactions between conjugated polymers and single-walled carbon nanotubes. *J. Phys. Chem. B* **106**, 3124 (2002).
18. R.J. Chen, Y. Zhang, D. Wang, and H. Dai: Noncovalent sidewall functionalization of single-walled carbon nanotubes for protein immobilization. *J. Am. Chem. Soc.* **123**, 3838 (2001).
19. E. Kymakis and G.A.J. Amaratunga: Single-wall carbon nanotube/conjugated polymer photovoltaic devices. *Appl. Phys. Lett.* **80**(1), 112 (2002).
20. R. Kreiter, A.W. Kleij, R.J.M. Gebbink, and G. van Koten: Dendritic catalysts. *Top. Curr. Chem.* **217**, 163 (2001).
21. D. Astruc and F. Chardac: Dendritic catalysts and dendrimers in catalysis. *Chem. Rev.* **101**, 2991 (2001).
22. R-B. Guo, W-W. Han, Z-L. Mo, L. Li, and C. Feng: Molecular dynamics study on the microstructure of dendrimers/graphite composites. *J. Mater. Res.* **27**(8), 1124 (2012).
23. E. Bustos, J.E. García, Y. Bandala, L.A. Godínez, and E. Juaristi: Enantioselective recognition of alanine in solution with modified gold electrodes using chiral PAMAM dendrimers G4.0. *Talanta* **78**(4–5), 1352 (2009).
24. Q-S. Hu, V. Pugh, M. Sabat, and L. Pu: Structurally rigid and optically active dendrimers. *J. Org. Chem.* **64**(20), 7528 (1999).
25. V.J. Pugh, Q-S. Hu, and L. Pu: The first dendrimer-based enantioselective fluorescent sensor for the recognition of chiral amino alcohols. *Angew. Chem. Int. Ed.* **39**(20), 3638 (2000).
26. L. Pu: Synthesis and study of binaphthyl-based chiral dendrimers. *J. Photochem. Photobiol., A* **155**, 47 (2003).
27. E. Canetta and G. Maino: Molecular dynamic analysis of the structure of dendrimers. *Nucl. Instrum. Methods Phys. Res., Sect. B* **213**, 71 (2004).
28. M. Grujicic, G. Cao, and W.N. Roy: Atomistic modeling of solubilization of carbon nanotubes by non-covalent functionalization with poly(p-phenylenevinylene-co-2,5-dioctoxy-m-phenylenevinylene). *Appl. Surf. Sci.* **227**, 349 (2004).
29. H. Sun: COMPASS: An ab initio force-field optimized for condensed-phase applications-overview with details on alkane and benzene compounds. *J. Phys. Chem. B* **102**(38), 7338 (1998).
30. H. Sun, P. Ren, and J.R. Fried: The COMPASS force field: Parameterization and validation for phosphazenes. *Comput. Theor. Polym. Sci.* **8**, 229 (1998).
31. M. Al-Haik, M.Y. Hussaini, and H. Garmestani: Adhesion energy in carbon nanotube-polyethylene composite: Effect of chirality. *J. Appl. Phys.* **97**(7), 074306 (2005).
32. J. Gou, B. Wang, Z-Y. Liang, and C. Zhang: Computational and experimental study of interfacial bonding of single-walled nanotube reinforced composites. *Comput. Mater. Sci.* **31**(3–4), 225 (2004).
33. J. Gou, Z-Y. Liang, C. Zhang, and B. Wang: Computational analysis of effect of single-walled carbon nanotube rope on molecular interaction and load transfer of nanocomposites. *Composites, Part B* **36**(6–7), 524 (2005).

https://doi.org/10.1557/jmr.2014.237 Published online by Cambridge University Press